

Structure and Dynamics of CO–Iron(II) Protoporphyrin IX in Dimethyl Sulfoxide[†]Randy W. Larsen,^{*,‡} Jim Murphy,[§] and Eric W. Findsen[§]

Departments of Chemistry, University of Hawaii at Manoa, 2545 The Mall, Honolulu, Hawaii 96822, and University of Toledo, Toledo, Ohio 43606

Received August 3, 1995[⊗]

In this report we examine the steady-state optical absorption, steady state and transient vibrational structure, and ligand rebinding kinetics of (CO)Fe^{II} protoporphyrin IX ((CO)Fe^{II}PPIX) in dimethyl sulfoxide (DMSO). Steady state optical absorption and resonance Raman spectra of this complex are characteristic of heme iron that is six-coordinate and low-spin. Absorption maxima are observed at 415 nm (Soret), 568 nm (α -band), and 535 nm (β -band), and vibrational bands are observed at 1370 cm⁻¹ (ν_4), 1496 cm⁻¹ (ν_3), 1551 cm⁻¹ (ν_{38}), 1584 cm⁻¹ (ν_2), and 1626 cm⁻¹ ($\nu_{C=C}$). The transient absorption difference spectrum subsequent to photolysis displays an absorption maximum at 433 nm and a minimum at 414 nm that decays biphasically with pseudo-first-order rate constants of $(2.11 \pm 0.024) \times 10^6$ s⁻¹ and $(2.29 \pm 0.036) \times 10^2$ s⁻¹. The corresponding transient resonance Raman spectrum displays vibrational bands at 1356 cm⁻¹ (ν_4), 1470 cm⁻¹ (ν_3), 1559 cm⁻¹ (ν_2), 1584 cm⁻¹ (ν_{37}), and 1618 cm⁻¹ ($\nu_{C=C}$). These results are consistent with the formation of a five-coordinate and high-spin transient species that is identical to the photolytic transient observed upon photolysis of the (DMSO)₂Fe^{II}PPIX complex (i.e., (DMSO)Fe^{II}PPIX). The decay of this transient species is consistent with the binding of a DMSO to the five-coordinate heme iron followed by substitution of a bound DMSO with CO.

Introduction

Metalloporphyrins represent a diverse class of molecules capable of catalyzing a wide range of chemical reactions. The diverse reactivity of porphyrins is exemplified by the abundance of porphyrins and porphyrin-like molecules that are utilized as active sites in proteins and enzymes. The most common porphyrin employed in biological chemistry is iron protoporphyrin IX (FePPIX) or heme. As an enzyme active site FePPIX can oxygenate organic substrates (monooxygenases), reduce dioxygen to water (oxidases), degrade hydrogen peroxide (peroxidases), reversibly transfer electrons (*b*- and *c*-type cytochromes), and reversibly transport and store oxygen (hemoglobin and myoglobin, respectively). To a large extent the nature of the coordination between the heme group and the protein modulates reactivity of the heme iron. For example, heme proteins responsible for reversible electron transfer contain heme iron that is six-coordinate and low-spin with axial ligand combinations derived from histidine, methionine, and/or lysine.^{1–5} Proteins and enzymes that activate or transport oxygen, on the other hand, have heme iron that is five-coordinate and high-spin with axial ligands derived from histidine, cysteine or tyrosine.^{6,7}

Understanding iron coordination chemistry in heme containing monooxygenases is of key interest in the design of

biomimetic systems as well as in elucidating fundamental reaction mechanisms associated with this class of enzyme. Electronic and structural interactions associated with anionic oxygen-donating ligands coordinated to iron porphyrins are of specific importance since these ligands may provide insights into the nature of iron–oxygen interactions associated with intermediates formed during monooxygenase catalysis.^{6,8} A vast majority of studies relating heme reactivity to iron axial ligation have focused on nitrogen-based ligands (e.g., imidazole, 2-methylimidazole, etc.), small diatomic molecules (e.g., O₂, CO, NO, etc.), and sulfur-based ligands.^{2–8} In contrast, studies of heme reactivity with organic-based oxygen ligands have been limited.^{9–11}

A potentially useful anionic oxygen donating ligand to heme is dimethyl sulfoxide (DMSO). The binding of sulfoxide ligands to ferric iron porphyrins has been demonstrated to occur through coordination of the sulfoxide oxygen to the central iron of the heme macrocycle.¹² This coordination is accompanied by a shift in $\nu_{S=O}$ of 110 cm⁻¹ to lower frequency, relative to the unbound molecule. Both Mossbauer and EPR spectra demonstrate that formation of the bis-DMSO ferric heme complex results in a heme iron that is high-spin. In fact, ferric bis-DMSO heme complexes are commonly employed as model complexes for six-coordinate and high-spin heme proteins.^{9–14}

It has recently been shown that the (DMSO)₂Fe^{II}PPIX complex forms a photolabile six-coordinate low-spin complex.^{15,16} We have previously found that photolysis of this

* Author to whom correspondence should be sent.

[†] R.W.L. would like to thank the donors of the Petroleum Research Fund, administered by the American Chemical Society, for supporting this work.

[‡] University of Hawaii at Manoa.

[§] University of Toledo.

[⊗] Abstract published in *Advance ACS Abstracts*, September 15, 1996.

- (1) Moore, G. R.; Pettigrew, G. W. *Cytochromes c-Evolutionary, Structural, and Physicochemical Aspects*; Springer-Verlag: Berlin, 1990.
- (2) Gouterman, M. in *The Porphyrins*; Dolphin, D., Ed.; Academic Press: New York, 1978; Vol. III.
- (3) Spiro, T. G. In *Iron Porphyrins*; Lever, A. B. P., Gray, H. B., Eds.; Addison-Wiley: Reading, MA, 1983.
- (4) Smith, K. *Porphyrins and Metalloporphyrins*; Elsevier: Amsterdam, 1975.
- (5) Hoard, J. L. In *Hemes and Heme Proteins*; Chance, B., Estabrook, R. W., Yonetani, T., Eds.; Academic Press: New York, 1966.
- (6) Ortiz de Montellano, P. *Cytochrome P-450: Structure, Mechanism, and Biochemistry*; Plenum Press: New York, 1986.
- (7) Schonbaum, G. R.; Chance, B. In *The Enzymes*, 3rd ed.; Boyer, P., Ed.; Academic Press: New York, 1976.
- (8) For reviews see: (a) Traylor, T. G. *Pure Appl. Chem.* **1991**, *63*, 265. (b) Jameson, G. B.; Ibers, J. A. *Comments Inorg. Chem.* **1983**, *2*, 97. (c) Morgan, B.; Dolphin, D. *Struct. and Bonding (Berlin)* **1987**, *64*, 115.
- (9) Ainscough, E. W.; Addison, A. W.; Dolphin, D.; James, B. R. *J. Am. Chem. Soc.* **1978**, *100*, 7585.
- (10) Otsuka, T.; Ohya, T.; Sato, M. *Inorg. Chem.* **1985**, *24*, 776.
- (11) Belal, R.; Momenteau, M.; Meunier, B. *New J. Chem.* **1989**, *13*, 853.
- (12) Mashiko, T.; Kastner, M. E.; Spartalian, K.; Scheidt, W. R.; Reed, C. A. *J. Am. Chem. Soc.* **1978**, *100*, 6354–6362.
- (13) Constant, L. A.; Davis, D. G. *Anal. Chem.* **1975**, *47*, 2253.
- (14) Bottomly, L. A.; Kadish, K. M. *Inorg. Chem.* **1981**, *20*, 1348.

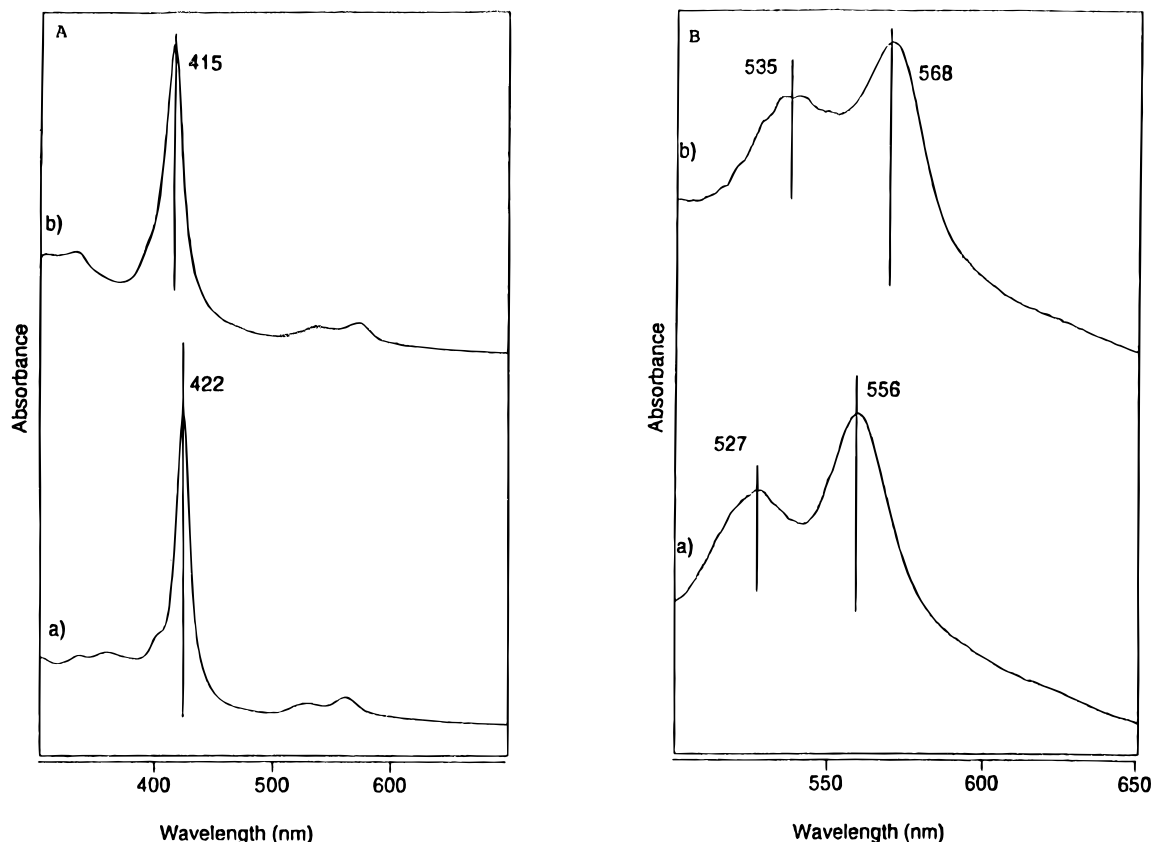


Figure 1. Panel A: Absorption spectra of (a) Fe^{II}PPIX in DMSO and (b) (CO)Fe^{II}PPIX in DMSO. Panel B: Expansion of the visible region for the traces described in panel A. Sample concentration: 5 μ M. Spectra were recorded in a sealed 1-cm quartz cuvette.

complex yields a five-coordinate, high-spin (DMSO)Fe^{II}PPIX complex that exhibits a relatively slow rate of recombination ($k_{\text{obs}} = \sim 2.0 \times 10^6 \text{ s}^{-1}$) when compared to recombination rates of nitrogen-based ligands. This slow recombination rate was attributed to strong dipolar interactions between the DMSO ligand and the transient five-coordinate high-spin heme.

In the current study we examine the vibrational structure, ligand photolysis and recombination of (CO)(DMSO)Fe^{II}PPIX in DMSO and compare these results with previous photolysis studies of the corresponding (DMSO)₂Fe^{II}PPIX complex. Carbon monoxide has been extensively employed to examine ligand binding dynamics in heme proteins and heme model complexes due to the high quantum yield for photolysis.^{2–8,17–20} Examination of the rates of ligand recombination and porphyrin vibrational structure subsequent to photodissociation of the (CO)Fe^{II}PPIX complex in DMSO provides an opportunity to examine the effects of ligand structure and electronic environment of highly polar oxygen-based ligands on heme reactivity. Our data demonstrates that photolysis of the (CO)(DMSO)Fe^{II}PPIX complex results in the formation of a five-coordinate complex with a red-shifted absorption spectrum, relative to the unphotolyzed species. In addition, biphasic ligand recombination is observed that is attributed to initial binding of a DMSO to the vacant sixth position followed by displacement of a coordinated DMSO by CO.

Table 1. Steady-State Absorption Maxima for Various Five- and Six-Coordinate Fe^{II}PPIX Complexes

complex	λ_{max} (nm)			Fe coord and spin-state	ref
	Soret	β - band	α - band		
(DMSO) ₂ Fe ^{II} PPIX	424	527	556	6-c, low	this work, 15
(Imid) ₂ Fe ^{II} PPIX ^a	426	529	559	6-c, low	16
(DMSO)(2MeIm)-Fe ^{II} PPIX	424	527	556	6-c, low	16
(2-MeIm)-Fe ^{II} PPIX ^b	431		559	5-c, high	29
(Imid) ₂ Fe ^{II} PPIX ^c	425	530	560	6-c, low	29
(pyridine) ₂ Fe ^{II} PPIX ^d	420	527	557	6-c, low	29
(OC ₆ H ₃ (3,4Me ₂)) ₂ Fe ^{II} PPDME ^e	434	562	593	5-c, high	9
Fe ^{II} PPDME–DMSO ^f	424	525	557	g	9
(1,2Me ₂ Im)(CO)Fe ^{II} PPDME	420	538	567	6-c, low	30
(DMSO)(CO)Fe ^{II} PPIX	415	535	568	6-c, low	this work
(DMSO)MP8 ⁱ	418	520	550	6-c, low	28
H93Y Mb ^h	427		560	5-c, high	27

^a In neat DMSO. ^b No β -band given. ^c In 1% (w/v) sodium dodecyl sulfate/0.01 M NaOH solution. ^d In pyridine/water (35% w/v). ^e (OC₆H₃(3,4Me₂)) = 3,4-dimethyl phenoxide, PPDME = protoporphyrin IX dimethyl ester. ^f Reported as “solvated” in DMSO. ^g No spin-state reported. ^h H93Y Mb = mutant myoglobin with the proximal histidine (His 93) replaced with a tyrosine as a catalase model. ⁱ MP8 = microperoxidase-8.

Materials and Methods

Hematin (Sigma), sodium dithionite (Aldrich), and DMSO (Spectral grade, Fisher) were used without further purification. Samples for steady-state and transient absorption studies were prepared by diluting hematin from a 3 mM stock solution (in DMSO) into a 1-cm quartz optical cuvette containing neat DMSO to give a final concentration of 5 μ M (determined using $\epsilon_{402 \text{ nm}} = 174 \text{ mM}^{-1} \text{ cm}^{-1}$).²¹ The sample was then sealed using a septum cap and purged with Ar or N₂ for 30 min. Solid sodium dithionite was then added and the samples were purged with Ar or N₂ for an additional 20 min. Optical absorption

- (15) Nalliah, R. E.; Findsen, E. W. *J. Raman. Spectrosc.* **1993**, *24*, 867.
 (16) Larsen, R. W.; Findsen, E. W.; Nalliah, R. E. *Inorg. Chim. Acta* **1995**, *234*, 101–107.
 (17) Marden, M. C.; Hazard, E. S.; Gibson, Q. H. *Biochemistry* **1986**, *25*, 2786–2792.
 (18) Traylor, T. G. *Acc. Chem. Res.* **1981**, *14*, 102–109.
 (19) Petrich, J. W.; Lambry, J.-C.; Kuczera, K.; Karplus, M.; Poyart, C.; Martin, J.-L. *Biochemistry* **1991**, *30*, 3975–3987.
 (20) Caldwell, K.; Noe, L. J.; Ciccone, J. D.; Traylor, T. G. *J. Am. Chem. Soc.* **1986**, *108*, 6150–6158.

- (21) Owens, J. W.; Robinson, J.; O'Connor, C. J. *Inorg. Chim. Acta* **1993**, *206*, 141.

Table 2. Resonance Raman Band Positions (in cm^{-1}) for Various Iron(II) Porphyrin Complexes

complex	spin state	ν_4	ν_3	ν_2	ν_{10}	$\nu_{\text{C=C}}$	ν_{38}/ν_{37}	ref
$(\text{DMSO})_2\text{Fe}^{\text{II}}\text{PPIX}$	ls	1368	1496	1584	1631		1557/...	15, this work
$(\text{CO})(\text{DMSO})\text{Fe}^{\text{II}}\text{PPIX}$	ls	1370	1496	1582		1626	1551/...	this work
$(\text{DMSO})\text{Fe}^{\text{II}}\text{PPIX}^a$	hs	1358	1469	1560	1521	1619	1521/e	15
$(\text{DMSO})\text{Fe}^{\text{II}}\text{PPIX}^b$	hs	1356	1470	1559	1523	1618	.../1584	this work
$(2\text{-MeIm})\text{Fe}^{\text{II}}\text{PPIX}^c$	hs	1357	1471	1562	1521	1622	1521/1583	29
$\text{Fe}^{\text{II}}\text{MP}^d$	is	1373	1506	1589	1642		1521/1620	25
$(\text{pyridine})_2\text{Fe}^{\text{II}}\text{MP}^d$	ls	1358	1490	1583	1620		1560/1620	25
$(\text{pyridine})(\text{CO})\text{Fe}^{\text{II}}\text{MP}^d$	ls	1371	1497	1588	1630		e	25

^a High power transient of the $(\text{DMSO})_2\text{Fe}^{\text{II}}\text{PPIX}$ complex. ^b High power transient of the $(\text{CO})(\text{DMSO})\text{Fe}^{\text{II}}\text{PPIX}$ complex. ^c In 1% (w/v) sodium dodecyl sulfate/0.01 M NaOH solution. ^d In CH_2Cl_2 . ^e Not reported.

spectra of the ferrous heme complex were obtained after a further 1-h incubation to insure complete reduction of the iron. The same samples were used for both the steady-state and transient absorption measurements. The $(\text{CO})\text{Fe}^{\text{II}}\text{PPIX}$ was prepared either by purging the ferrous heme complex with CO (Matheson) gas for 10 min or by purging a solution containing $\text{Fe}^{\text{II}}\text{PPIX}$ with CO followed by addition of dithionite. Both procedures yielded identical results.

Nanosecond transient absorption and resonance Raman data were obtained with instrumentation described in detail elsewhere.^{15,16} Nanosecond transient absorption data were obtained by exciting the sample in a 1-cm quartz optical cuvette with a 10 ns pulse from a frequency doubled Nd:YAG laser (Continuum SureLite II, 532 nm, 3.0 mJ/pulse). The change in absorbance was monitored by focusing the the arc of a 75-W Xe arc lamp through the sample and overlapping with the excitation pulse. The light passing through the sample was imaged onto the entrance slit of a Spex 1480 double monochromator and detected with a Hamamatsu R928 photomultiplier tube. The resulting signal was amplified with a preamplifier of our own design and digitized using a Tektronix RTD 710A 200 MHz transient digitizer. The data were analyzed using nonlinear least-squares methods using Enzfitter software.

Raman spectra were acquired using a Quantel YG571C pico/nano Nd:YAG laser operating in nanosecond pulse mode producing pulses with a nominal width of 10 ns and a repetition rate of 9 Hz. The frequency tripled fundamental (355 nm) was focused into a Raman shift cell containing hydrogen gas. The required excitation wavelength was isolated using dichroic reflectors and focused on the sample in a back scattering geometry using either cylindrical or spherical optics. The scattered radiation was collected and focused through a polarization scrambler into a 1.5 m spectrograph (Sopra) and on to a gated intensified diode array detector (Princeton Instruments IRY-700). Spectra were calibrated by referencing to the Raman spectrum of neat indene. Laser power at the sample was modulated either by changing the focus of the laser or by the use of neutral density filters.

Steady-state absorption spectra were obtained using either a Milton Roy Spectronic 3000 diode array or Varian Cary 5 spectrophotometer. Optical absorption spectra were obtained before and after transient absorption/Raman measurements to insure sample integrity.

Results and Discussion

Steady-State Characterization of $(\text{DMSO})_2\text{Fe}^{\text{II}}\text{PPIX}$ and $(\text{CO})(\text{DMSO})\text{Fe}^{\text{II}}\text{PPIX}$ Complexes. The optical absorption of the $(\text{DMSO})_2\text{Fe}^{\text{II}}\text{PPIX}$ and $(\text{CO})(\text{DMSO})\text{Fe}^{\text{II}}\text{PPIX}$ complexes are displayed in Figure 1. The optical absorption spectrum of the $(\text{DMSO})_2\text{Fe}^{\text{II}}\text{PPIX}$ displays a Soret maximum at 424 nm with visible bands located at 556 nm (α -band) and 527 nm (β -band) consistent with previous results.^{15,16} The positions of these bands are characteristic of six-coordinate, low-spin heme complexes (see Table 1). Exposure of the $(\text{DMSO})_2\text{Fe}^{\text{II}}\text{PPIX}$ to CO results in a hypsochromic shift in the Soret band to 415 nm and bathochromic shifts in both the α - and β -bands to 568 and 535 nm, respectively (Figure 1, trace b). The shifts are characteristic of CO binding to ferrous hemes and are due to electron back-donation from the reduced iron to an antibonding orbital on CO.²⁻⁵ Since Fe^{II} porphyrins do not form bis-CO complexes the species formed is a $(\text{CO})(\text{DMSO})\text{Fe}^{\text{II}}\text{PPIX}$ complex.²⁻⁵

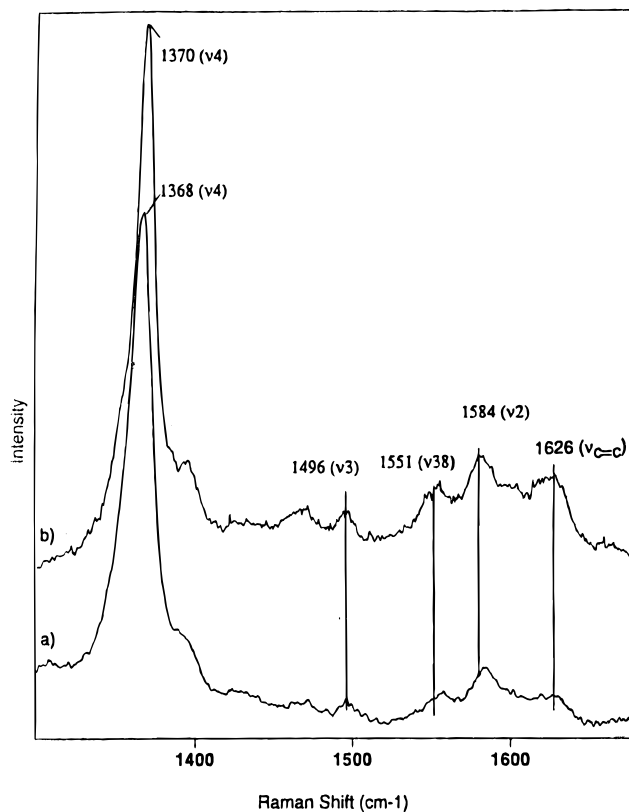


Figure 2. Resonance Raman spectra of (a) $\text{Fe}^{\text{II}}\text{PPIX}$ in DMSO and (b) $(\text{CO})\text{Fe}^{\text{II}}\text{PPIX}$ in DMSO obtained under low power conditions (i.e., 1 mJ/pulse, 416 nm excitation ($(\text{CO})\text{Fe}^{\text{II}}\text{PPIX}$) and 436 nm excitation ($(\text{DMSO})_2\text{Fe}^{\text{II}}\text{PPIX}$), 10 ns pulse width).

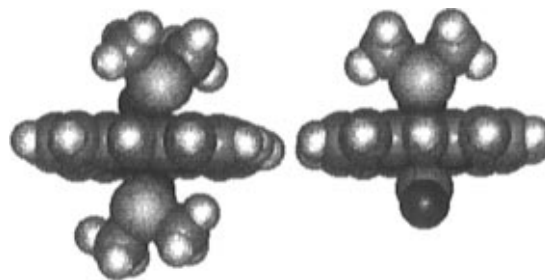


Figure 3. Geometry optimized space filling model of $(\text{DMSO})_2\text{Fe}^{\text{II}}\text{PPIX}$ (left) and $(\text{CO})(\text{DMSO})\text{Fe}^{\text{II}}\text{PPIX}$ (right) complexes obtained using a modified MM+ molecular mechanics application with HyperChem. The modified MM+ force field is described in ref 24.

The steady state resonance Raman spectrum of the $(\text{DMSO})_2\text{Fe}^{\text{II}}\text{PPIX}$ and $(\text{CO})(\text{DMSO})\text{Fe}^{\text{II}}\text{PPIX}$ complexes are shown in Figure 2 and the peak positions are tabulated in Table 2. The resonance Raman spectrum of the $(\text{DMSO})_2\text{Fe}^{\text{II}}\text{PPIX}$ displays vibrational bands at $1368\text{ cm}^{-1}(\nu_4)$, $1496\text{ cm}^{-1}(\nu_3)$, $1551\text{ cm}^{-1}(\nu_{38})$, and $1584\text{ cm}^{-1}(\nu_2)$ (Figure 2, trace a). The corresponding resonance Raman spectrum of the $(\text{CO})(\text{DMSO})\text{Fe}^{\text{II}}$

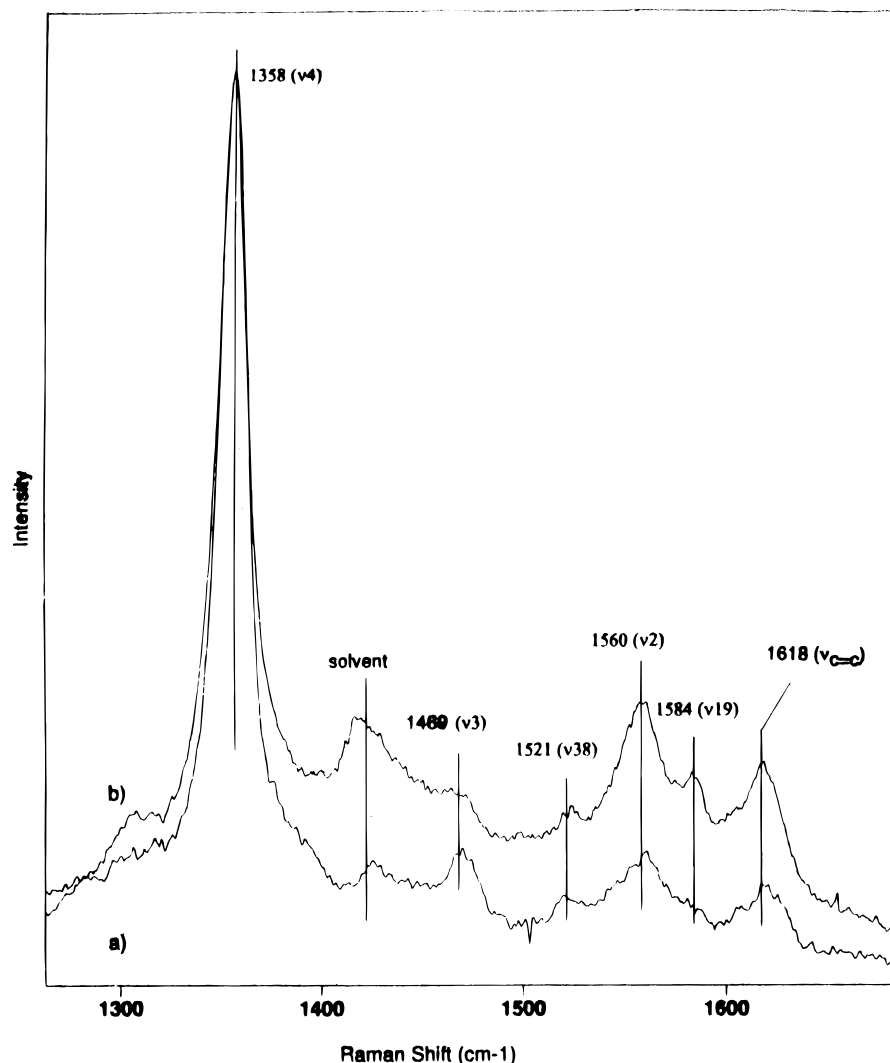


Figure 4. Transient resonance Raman spectra of (a) Fe^{II}PPIX in DMSO and (b) (CO)Fe^{II}PPIX in DMSO. Spectra were obtained under high power conditions (i.e., 10 mJ/pulse). Excitation conditions are the same as in Figure 2.

PPIX complex displays vibrational bands at 1370 cm⁻¹ (ν_4), 1496 cm⁻¹ (ν_3), 1551 cm⁻¹ (ν_{38}), 1582 cm⁻¹ (ν_2), and 1626 cm⁻¹ ($\nu_{C=C}$) (Figure 2, trace b). We note the presence of a small amount of the photolytic transient as judged by a shoulder on the low-frequency side of ν_4 and a band at 1469 cm⁻¹ assigned as ν_3 for the five-coordinate high-spin state (see next section). Previous studies have shown that the positions of the high frequency skeletal vibrations (above ~ 1450 cm⁻¹) exhibit an inverse correlation with porphyrin core size.^{22,23} The position of ν_2 and ν_3 associated with the (DMSO)₂Fe^{II}PPIX and (CO)-(DMSO)Fe^{II}PPIX complexes are consistent with a heme center to N distance of 1.999 ± 0.01 Å for both species. This value is similar to that observed for other six-coordinate, low-spin ferrous heme complexes in which the iron atom lies within the plane of the porphyrin ring.²⁴ Preliminary molecular modeling calculations using an MM+ force field modified to include parameters for six-coordinate low-spin metalloporphyrins also show that the iron atom lies within the plane of the porphyrin ring for both the (DMSO)₂Fe^{II}PPIX and the (CO)(DMSO)Fe^{II}PPIX complexes (see Figure 3).²⁴

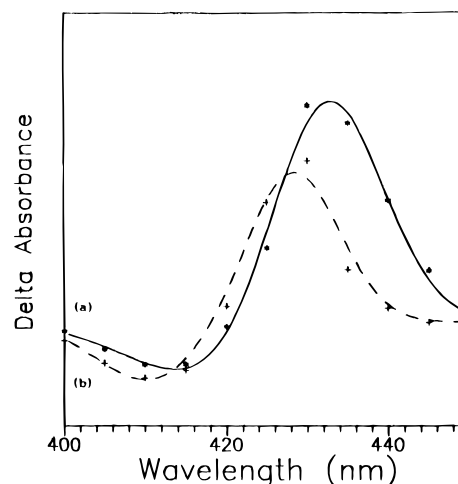


Figure 5. Transient absorption difference spectra reconstructed from single wavelength transient absorption data. Time scales are (a) ~ 30 ns and (b) $2 \mu\text{s}$ subsequent to photolysis. The smooth line is a best fit to the difference between two Lorentzian band shapes. Difference spectra are postflash minus preflash. Sample conditions are described in Figure 1.

The frequency of ν_4 is also known to be sensitive to the amount of electron density localized on the central metal.^{25,26} Thus the position of ν_4 is an indication of the metal oxidation state and degree of π -back-bonding between the metal d_{xy} and

(22) Parthasarathi, N.; Hansen, C.; Yamaguchi, S.; Spiro, T. G. *J. Am. Chem. Soc.* **1987**, *109*, 3865–3871.

(23) Spiro, T. G.; Stong, J. D.; Stein, K. M. *J. Am. Chem. Soc.* **1979**, *101*, 2648.

(24) Munro, O. Q.; Bradley, J. C.; Hancock, R. D.; Marques, H. M.; Marsicano, F.; Wade, P. W. *J. Am. Chem. Soc.* **1992**, *114*, 7218–7230.

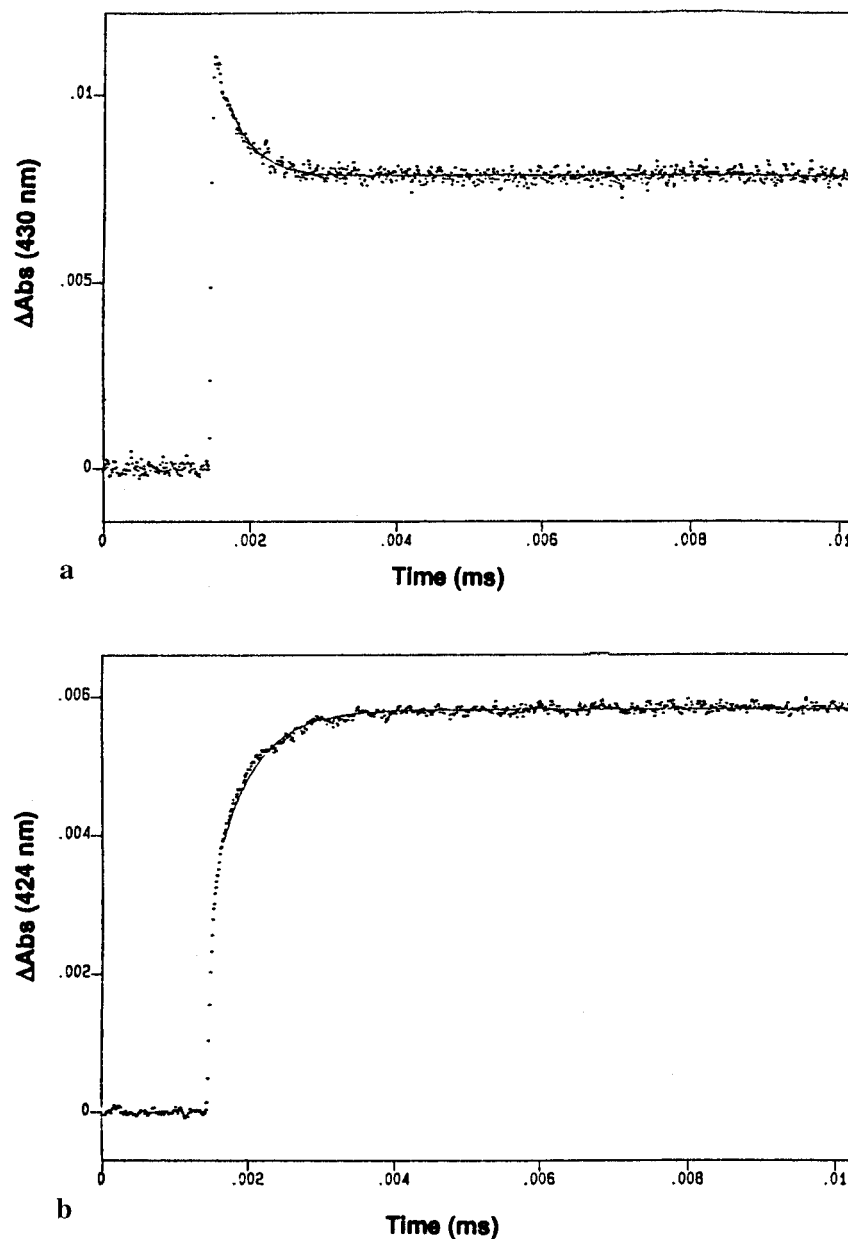


Figure 6. Representative single wavelength transient absorption data of the $(\text{CO})(\text{DMSO})\text{Fe}^{\text{II}}\text{PPIX}$ complex at (a) 435 nm, and (b) 424 nm obtained on a 10 μs time scale with 10 ns/point resolution. Sample conditions are described in Figure 1.

d_{yz} orbitals and the porphyrin π^* orbital. This mode exhibits an increase in Raman shift as the degree of back bonding increases. The position of ν_4 (1368 cm^{-1}) in the resonance Raman spectrum of $(\text{DMSO})_2\text{Fe}^{\text{II}}\text{PPIX}$ complex is intermediate between weak π -accepting ligands such as imidazole (ν_4 for $(\text{imidazole})_2\text{Fe}^{\text{II}}\text{PPIX}$ is $\sim 1356\text{ cm}^{-1}$) and strong π -accepting ligands such as CO (ν_4 for $(\text{CO})(\text{pyridine})\text{Fe}^{\text{II}}(\text{mesoporphyrin})$ is $\sim 1371\text{ cm}^{-1}$).^{23,25,26} This finding suggests a significant degree of back-bonding occurs between bound DMSO and the heme iron, presumably through a π^* orbital associated with DMSO. The shift in ν_4 to higher frequency upon formation of the $(\text{CO})(\text{DMSO})\text{Fe}^{\text{II}}\text{PPIX}$ complex is consistent with a further increase in back-donation due to the presence of the stronger π -accepting CO ligand and supports the conclusion that the π -accepting ability of DMSO is less than that of CO.

Transient Resonance Raman Studies of the $(\text{DMSO})_2\text{Fe}^{\text{II}}\text{PPIX}$ and $(\text{CO})(\text{DMSO})\text{Fe}^{\text{II}}\text{PPIX}$ Complexes. Nalliah

(25) Spiro, T. G.; Burke, J. M. *J. Am. Chem. Soc.* **1976**, *98*, 5482–5489.
 (26) Jacob, S. W.; Rosenbaum, E. E.; Wood, D. C. *Dimethyl Sulphoxide*; Marcel Dekker, Inc.: New York, 1971.

and Findsen¹⁵ have recently shown that the resonance Raman spectrum of the $(\text{DMSO})_2\text{Fe}^{\text{II}}\text{PPIX}$ complex obtained with high laser powers exhibits vibrational bands quite distinct from those obtained under low-power conditions and are consistent with the reversible formation of a five-coordinate, high-spin $(\text{DMSO})\text{Fe}^{\text{II}}\text{PPIX}$ complex. The resonance Raman spectrum of the $(\text{CO})(\text{DMSO})\text{Fe}^{\text{II}}\text{PPIX}$ complex obtained under high power conditions is also quite distinct relative to the spectrum obtained using low laser powers. In addition the species generated under high power conditions displays a high frequency vibrational spectrum identical to that of the $(\text{DMSO})_2\text{Fe}^{\text{II}}\text{PPIX}$ complex obtained under high power conditions (differences in relative intensities are due to differences in excitation wavelength; 416 nm for the $(\text{CO})(\text{DMSO})\text{Fe}^{\text{II}}\text{PPIX}$ complex and 436 nm for the $(\text{DMSO})_2\text{Fe}^{\text{II}}\text{PPIX}$ complex) (Figure 4). The high frequency resonance Raman spectrum of the $(\text{DMSO})_2\text{Fe}^{\text{II}}\text{PPIX}$ complex obtained with high laser powers ($\sim 10\text{ mJ/pulse}$) displays vibrational bands at 1358 cm^{-1} (ν_4), 1469 cm^{-1} (ν_3), 1521 cm^{-1} (ν_{38}), 1560 cm^{-1} (ν_2), 1584 cm^{-1} (ν_{19}), and 1618 cm^{-1} ($\nu_{\text{C=C}}$). The corresponding spectrum of the $(\text{CO})(\text{DMSO})\text{Fe}^{\text{II}}\text{PPIX}$

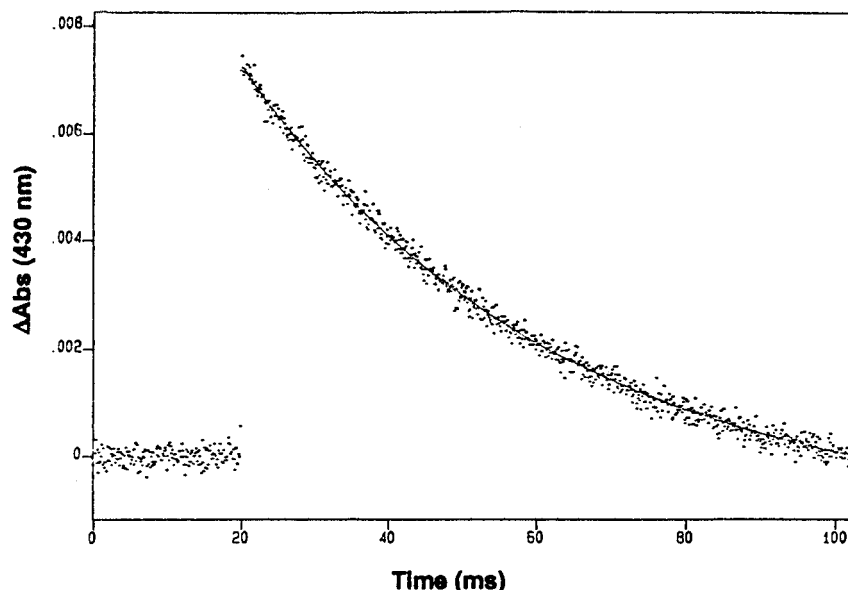


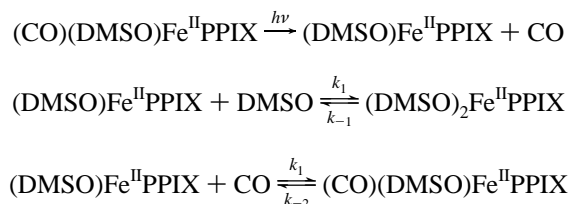
Figure 7. Single wavelength transient absorption data of the (CO)(DMSO)Fe^{II}PPIX complex at 430 nm obtained on a 100 ms time scale with 1 μ s/point resolution. Solid lines are best fits using a single exponential function. Sample conditions are described in Figure 1.

obtained under similar conditions displays modes at 1356 cm^{-1} (ν_4), 1470 cm^{-1} (ν_3), 1523 cm^{-1} (ν_{38}), 1559 cm^{-1} (ν_2), 1584 cm^{-1} (ν_{19}), and 1619 cm^{-1} ($\nu_{C=C}$). Examination of the positions of the high frequency vibrational modes ν_2 and ν_3 show that the porphyrin core size associated with the transient species is 2.055 ± 0.01 Å. The core size of the transient species is similar to that of other five coordinate high-spin heme complexes such as (2-MeIm)Fe^{II}PPIX (2.047 Å) and (2-MeIm)Fe^{II} (tetraphenylporphyrin) (2.043 Å).^{25,26}

Transient Absorption Studies of (DMSO)₂Fe^{II}PPIX and (CO)(DMSO)Fe^{II}PPIX Complexes. Previous resonance Raman and transient absorption studies have demonstrated that the (DMSO)₂Fe^{II}PPIX complex is photolabile.^{15,16} The photolysis product displays an absorption difference spectrum with an absorption maximum at 435 nm and a minimum at 423 nm. These studies have further shown that the decay of the (DMSO)-Fe^{II}PPIX transient occurs monophasically by rebinding a DMSO ligand to the vacant sixth-coordination site. The observed rate constant for this rebinding was found to be on the order of 2×10^6 s⁻¹. This relatively slow rate of recombination was attributed, in part, to the repulsion between the d_{z^2} orbital of the transient high-spin iron and the partial negative charge on the sulfoxide oxygen arising from the large dipole moment associated with the O=S bond. We point out here that steric factors may also contribute to the slow DMSO binding to the (DMSO)Fe^{II}PPIX complex. The atoms in the DMSO molecule are arranged in a tetrahedral geometry with the sulfur atom at the center. The two methyl groups, the oxygen atom, and a nonbonding electron pair occupy the apex position.²⁷ The effect of this tetrahedral arrangement on binding to heme is depicted in Figure 3. Steric repulsion is likely to occur between the porphyrin ring and the methyl groups of DMSO as well as between the lone pair electrons localized on the sulfur atom. These steric interactions will also contribute a significant barrier to recombination of DMSO to the (DMSO)Fe^{II}PPIX complex.

Photolysis of the (CO)(DMSO)Fe^{II}PPIX yields an initial transient species which exhibits an absorption maximum at 433 nm and absorption minimum at 414 nm (Figure 5, trace a). This species decays biphasically with rate constants of $(2.11 \pm 0.024) \times 10^6$ s⁻¹ and $(2.29 \pm 0.036) \times 10^2$ s⁻¹. Single wavelength transient absorption decays obtained at various wavelengths are displayed in Figure 6 (10 μ s time scale) and Figure 7 (100 ms time scale). The transient absorption difference spectrum of the photoproduct obtained immediately after photolysis (~ 30 ns trigger delay in our instrument) is characteristic of a five-coordinate and high-spin heme iron. This difference spectrum can be recreated by subtracting the equilibrium absorption spectrum of the (CO)(DMSO)Fe^{II}PPIX complex from that obtained from photodissociation of the (DMSO)₂Fe^{II}PPIX complex suggesting that the photolytic transient consists of a five-coordinate high-spin (DMSO)Fe^{II}PPIX complex.

In contrast, the corresponding transient absorption difference spectrum obtained 2 μ s subsequent to photolysis reveals a new species with a maximum at 426 nm and a minimum at 410 nm (Figure 5, trace b) that ultimately decays back to the starting complex. This difference spectrum can be recreated by subtracting the equilibrium (CO)(DMSO)Fe^{II}PPIX spectrum from that of the equilibrium (DMSO)₂Fe^{II}PPIX complex. These results are consistent with a mechanism for ligand recombination described as follows:



In this scheme the initial event associated with ligand recombination to the (DMSO)Fe^{II}PPIX complex is the binding of a DMSO to the vacant sixth coordination site at the heme iron with a pseudo-first-order rate constant, k_1 , of $(2.11 \pm 0.024) \times 10^6$ s⁻¹. Scaling this value to the concentration of ligand gives a second-order rate constant of $(1.5 \pm 0.024) \times 10^5$ M⁻¹ s⁻¹. The six-coordinate (DMSO)₂Fe^{II}PPIX complex is in equilibrium with the five-coordinate (DMSO)Fe^{II}PPIX complex with an equilibrium constant $K = (k_1)/(k_{-1})$. The photodisso-

(27) Abachi, S.-I.; Nagano, S.; Watanabe, Y.; Ishimori, K.; Morishima, I. *Bioch. Biophys. Res. Commun.* **1991**, 138–144.

(28) Pande, J.; Kinnally, K.; Thallum, K. K.; Verma, B. C.; Myer, Y. P.; Rechsteiner, L.; Bosshard, H. R. *J. Prot. Chem.* **1987**, 6, 320.

(29) Desbois, A.; Henry, Y.; Lutz, M. *Bioch. Biophys. Acta* **1984**, 785, 148.

(30) Traylor, T. G.; Magde, D.; Taube, D. J.; Jongeward, K. A.; Bandyopadhyay, D.; Luo, J.; Walda, K. N. *J. Am. Chem. Soc.* **1992**, 114, 417.

Table 3. Rate and Equilibrium Constants for Selected (L)(L')Fe^{II}(porphyrin) Complexes

complex	k_2 (M ⁻¹ s ⁻¹)	k_{-2} (s ⁻¹)	K (M ⁻¹)	ref
(DMSO) ₂ Fe ^{II} PPIX	1.5×10^5	6.92	2.2×10^4	this work
(pyridine) ₂ Fe ^{II} TPP ^a	4.7×10^8	1.2×10^4	3.7×10^4	32
(Imid)(1MeIm)Fe ^{II} TPP ^b	1.8×10^8	1.5×10^3	1.2×10^5	32
(piperidine)(pyridine)Fe ^{II} TPP ^c	3.7×10^8	7.5×10^3	4.9×10^4	32
(Imid) ₂ Fe ^{II} TPP ^d	1.9×10^8	1.7×10^3	1.1×10^5	32

^a Pyridine-chelated tetraphenylporphyrin in toluene. ^b Chelated 1-methylimidazole (1MeIm) in toluene. ^c Pyridine-chelated tetraphenylporphyrin in toluene. ^d Imidazole-chelated (Imid) tetraphenylporphyrin in toluene.

ciated CO can then rebind to a vacant sixth coordination site formed by the equilibrium described above with a pseudo-first-order rate constant (CO exchange rate) of $(2.29 \pm 0.036) \times 10^2$ s⁻¹ (second-order rate constant of $(4.58 \pm 0.036) \times 10^2$ M⁻¹ s⁻¹ after scaling to CO concentration³¹) resulting in the regeneration of the (CO)(DMSO)Fe^{II}PPIX complex.

Lavalette *et al.*³² have previously utilized photolysis of (CO)Fe^{II}TPP-B (TPP = tetraphenylporphyrin, B = covalently attached base) in the presence of an exogenous ligand, L, as a probe for k_{-1} in a series of (L)Fe^{II}TPP-B complexes by assuming that k_{-1} is the rate limiting step in CO rebinding. This was accomplished using

$$1/R = (1/k_{-1})(k_1/k_2)$$

where R is the CO exchange rate. In the present study we can not determine k_2 since this rate constant describes CO rebinding

- (31) The solubility of CO in DMSO was estimated using the solubility of O₂ found in ref 26.
 (32) Lavalette, D.; Tetreau, C.; Momenteau, M. *J. Am. Chem. Soc.* **1979**, *101*, 5395.

to a bare five-coordinate heme and we have been unable to prepare a stable five-coordinate (DMSO)Fe^{II}PPIX complex. However, the data presented by Lavalette *et al.*³² and Traylor^{8a} suggest that k_2 is not significantly affected by the nature of the proximal base. Thus using k_2 from Lavalette *et al.* ($\sim 5 \times 10^6$ M⁻¹ s⁻¹) for nitrogenous base complexes and k_1 (1.5×10^5 M⁻¹ s⁻¹) and R (2.29×10^2 s⁻¹) determined in our work gives an estimate of 6.92 s⁻¹ for k_{-1} . Using this value gives an estimate of 2.2×10^4 M⁻¹ for the equilibrium constant, K. Within the approximations used here the dissociation rate for DMSO is found to be considerably lower than the corresponding nitrogenous bases (e.g., imidazole, pyridine, etc.) (see Table 3). The low dissociation rate for DMSO relative to nitrogenous bases may be due to additional stabilization of the bound ligand through π -back-bonding to the iron (as observed in the Raman data). In fact, the calculated dissociation rate of the (DMSO)₂Fe^{II}-PPIX more closely resemble the off rate of O₂ from chelated protohemes and hemoglobin (~ 47 s⁻¹ and 17 s⁻¹, respectively).^{8a}

In summary, the data presented here demonstrates that the (CO)(DMSO)Fe^{II}PPIX complex is low-spin and photolabile. Upon photolysis a five-coordinate high-spin (DMSO)Fe^{II}PPIX complex is formed which is spectroscopically identical to the species generated by photolysis of the (DMSO)₂Fe^{II}PPIX complex. In the presence of carbon monoxide this transient species decays via a two-step ligation mechanism to regenerate the parent (CO)(DMSO)Fe^{II}PPIX complex. The first step involves the binding of a DMSO ligand to the sixth coordination site to form a (DMSO)₂Fe^{II}PPIX complex. The second step is the slow ligand displacement of an axial DMSO ligand by CO to reform the parent complex. These results provide an excellent framework for future studies to explore the nature of highly polar oxygen based molecules as heme ligands.

IC950998C